NANO LETTERS

2007
Vol. 7, No. 6
1551−1555

Local Magnetic Properties of a Monolayer of Mn_{12} Single Molecule Magnets

Z. Salman,*[†,‡,§] K. H. Chow,[||] R. I. Miller,[§] A. Morello,[⊥] T. J. Parolin,[#] M. D. Hossain,[⊥] T. A. Keeler,[⊥] C. D. P. Levy,[§] W. A. MacFarlane, G. D. Morris,[§] H. Saadaoui,[⊥] D. Wang,[⊥] R. Sessoli,[¶] G. G. Condorelli,[∞] and R. F. Kiefl[§,⊥]

Clarendon Laboratory, Department of Physics, Oxford University, Parks Road, Oxford OX1 3PU, U.K., ISIS Facility, Rutherford Appleton Laboratory, Chilton, Oxfordshire, OX11 0QX, U.K., TRIUMF, 4004 Wesbrook Mall, Vancouver, British Columbia V6T 2A3, Canada, Department of Physics, University of Alberta, Edmonton, Alberta T6G 2G7, Canada, Department of Physics and Astronomy, University of British Columbia, Vancouver, British Columbia V6T 1Z1, Canada, Department of Chemistry, University of British Columbia, Vancouver, British Columbia V6T 1Z1, Canada, Dipartimento di Chimica, Universitá di Firenze & INSTM, via della Lastruccia 3, 50019 Sesto Fiorentino, Italy, and Dipartimento di Scienze Chimiche, Universitá di Catania & INSTM UdR di Catania, viale A. Doria 6, 95125 Catania, Italy

Received February 14, 2007; Revised Manuscript Received April 16, 2007

ABSTRACT

The magnetic properties of a monolayer of Mn_{12} single molecule magnets grafted onto a silicon (Si) substrate have been investigated using depth-controlled β-detected nuclear magnetic resonance. A low-energy beam of spin-polarized radioactive ^{8}Li was used to probe the local static magnetic field distribution near the Mn_{12} monolayer in the Si substrate. The resonance line width varies strongly as a function of implantation depth as a result of the magnetic dipolar fields generated by the Mn_{12} electronic magnetic moments. The temperature dependence of the line width indicates that the magnetic properties of the Mn_{12} moments in this low-dimensional configuration differ from bulk Mn_{12}.

Single molecule magnets (SMMs)[1] are molecules which contain a small number of magnetic ions with large magnetic interactions between them ($J \sim 10-100$ K). The magnetic core of each molecule is surrounded by organic or inorganic ligands. Since the molecules are magnetically isolated, they form at low temperature a lattice of very weakly interacting spins. Practical application of SMMs as molecular scale units for information storage[2,3] or "qubits" for quantum computation[4−7] requires addressing individual molecules, which may be realized in principle by depositing a monolayer of molecules on a suitable substrate. Methods to deposit suitably derivatized Mn_{12}-type clusters on gold[8−11] and Si[12,13] have been developed recently, opening up exciting possibilities for applications of SMMs for information storage on a single molecule and for the investigation of the quantum behavior of isolated spins, such as quantum tunneling of the magnetization (QTM),[1,14−16] topological quantum phase interference,[17,18] and quantum coherence.[19−21] Unfortunately, the small quantity of magnetic material in the case of a monolayer (or submonolayer[11]) implies that it is virtually impossible to accurately determine their magnetic properties with conventional bulk techniques, such as SQUID magnetometry or conventional nuclear magnetic resonance (NMR). However, a new technique, namely, depth-resolved β-detected NMR (β-NMR), which has $\approx 10^{13}$ orders of magnitude higher sensitivity compared to conventional NMR, is well-suited for studying such systems.[22−26]

In this paper we report β-NMR measurements of the magnetic moment of Mn_{12} molecules which are grafted as a monolayer on a Si substrate. The experiments were performed using a low-energy beam of highly polarized radioactive ^{8}Li, implanted into the Si substrate just below the Mn_{12} monolayer. The strength and distribution of the magnetic dipolar fields from the Mn_{12} moments determine the shape of the ^{8}Li NMR resonance. Interestingly, the

* Corresponding author. E-mail: z.salman1@physics.ox.ac.uk.
† Clarendon Laboratory, Department of Physics, Oxford University.
‡ ISIS Facility, Rutherford Appleton Laboratory.
§ TRIUMF.
|| Department of Physics, University of Alberta.
⊥ Department of Physics and Astronomy, University of British Columbia.
Department of Chemistry, University of British Columbia.
¶ Dipartimento di Chimica, Universitá di Firenze & INSTM.
∞ Dipartimento di Scienze Chimiche, Universitá di Catania & INSTM.

10.1021/nl070366a CCC: $37.00
Published on Web 05/08/2007

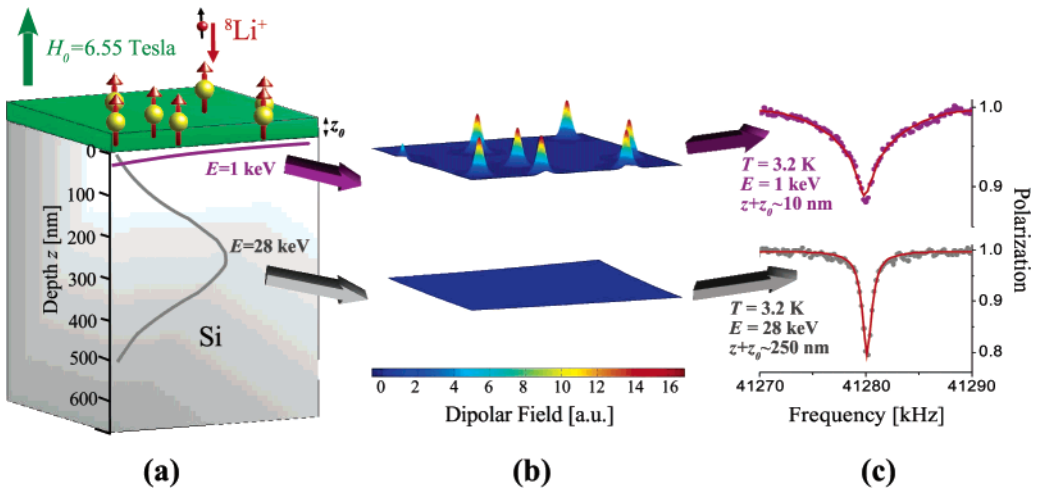

Figure 1. (a) A schematic of sample **1** where the Mn_{12} molecules are grafted on a Si substrate. The stopping profiles of ^{8}Li in Si at E = 1 and 28 keV are also shown (purple and gray lines, respectively). (b) The simulated dipolar fields from the Mn_{12} monolayer calculated near the surface (top) and deep within (bottom) the Si substrate (arbitrary units). (c) The measured β-NMR spectra from sample **1** in an applied magnetic field $H_0 = 6.55$ T at $T = 3.2$ K. The top spectrum is for $E = 1$ keV and the bottom for $E = 28$ keV. The solid lines are fits to the calculated resonance line shape (see text).

temperature dependence of the signal deviates significantly from that expected from the measured magnetization for bulk Mn_{12}. This is evidence that the interactions characterizing Mn_{12} in this two-dimensional (2D) configuration are different from those in the bulk.

Magnetic resonance techniques have been used extensively to study the magnetic properties of SMMs in the bulk. In particular, conventional NMR[27−31] and muon spin relaxation[27,28,32,33] (μSR) have been used to measure the molecular spin dynamics in both the thermally activated regime and the quantum tunneling regime. β-NMR is a closely related technique, where one measures the nuclear magnetic resonance and relaxation of ^{8}Li, a spin $I = 2$ nucleus with a small electric quadrupole moment $Q = +33$ mB and gyromagnetic ratio $\gamma = 6.301$ MHz/T. The radioactive $^8Li^+$ beam is produced at the isotope separator and accelerator (ISAC) at TRIUMF. It is then polarized using a collinear optical pumping method and implanted into the sample. Since the implantation energy can be varied between 0.9 and 28 keV, corresponding to an average implantation depth in Si of 1−250 nm, depth-resolved β-NMR measurements are possible. As in any form of NMR, the time evolution of the nuclear polarization is the quantity of interest. It can be measured through the β-decay asymmetry, where an electron is emitted preferentially opposite to the direction of the nuclear polarization at the time of decay[34] and detected by appropriately positioned scintillation counters. As noted above, this method of detection is dramatically more sensitive than conventional NMR and makes β-NMR suitable for studies of ultrathin films and nanostructures.[22,23] The nuclear resonance in a static magnetic field, $\mathbf{H_0} = H_0\hat{z}$, can be detected by measuring the time averaged nuclear polarization along $\hat{z}$, $p_z(\nu)$, as a function of the frequency ν of a small (∼1 G) oscillating perpendicular magnetic field, $\mathbf{H_1}(t) = H_1 \cos(2\pi\nu t)\hat{x}$. A loss of polarization occurs when ν matches the Larmor frequency of the nuclear spins of the ^{8}Li, a value that is given by the product of γ and the local field it experiences. Hence, the position and shape of the resonance(s) signals provide detailed information on the distribution of static local magnetic fields.

The experiments reported here were performed on two different samples. Sample **1** was prepared using a three-step process:[12] (1) grafting of methyl ester of 10-undecanoic acid on a H-terminated Si(100) substrate, (2) hydrolysis of the ester group, and (3) ligand exchange between $[Mn_{12}O_{12}(OAc)_{16}(H_2O)_4]\cdot 4H_2O\cdot 2AcOH$ and the grafted undecanoic acid to anchor the Mn_{12} SMMs to the organic layer. A schematic of sample **1** is shown in Figure 1a. Sample **2** is an identically prepared Si substrate, i.e., following step 1 only. It is used as a control sample in order to confirm that the effects measured in **1** are solely due to the Mn_{12}. The samples were mounted in an ultrahigh vacuum environment on a cold finger cryostat. The resonance lines of ^{8}Li were measured at various temperatures and implantation energies in both samples in an external magnetic field $H_0 = 6.55$ T, perpendicular to the Si surface.

The β-NMR spectra were measured by implanting the ^{8}Li beam at different energies in the Si substrate *below* the Mn_{12} monolayer. An example of the stopping profile of the implanted ^{8}Li at two different energies is shown in Figure 1a. At $E = 1$ keV, where most of the ^{8}Li stop within 10 nm of the Si surface, the dipolar field from the Mn_{12} moments is large, as illustrated in Figure 1b. However, at $E = 28$ keV the average ^{8}Li implantation depth is ∼250 nm, and the dipolar field at this depth is negligible; hence, the local field experienced by the ^{8}Li is simply the applied uniform $\mathbf{H_0}$. As a result the measured resonance line at 1 keV is significantly broadened compared to that measured at 28 keV, as clearly seen in Figure 1c at $T = 3.2$ K. Furthermore, the resonance measured in sample **2** at $E = 28$ keV and $T = 3.2$ K is identical to that measured in sample **1** under the same conditions, and the broadening observed in sample **2** is much smaller at $E = 1$ keV. This demonstrates that low-energy β-NMR spectroscopy is sensitive to the magnetization of the Mn_{12} monolayer. In particular, the ^{8}Li nuclei implanted into sample **1** at low E, and hence stopping close to the Mn_{12}

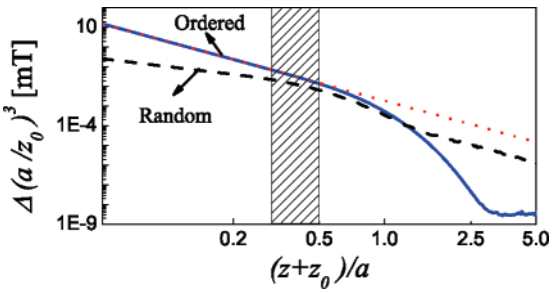

Figure 2. The simulated value of Δ as a function of distance from a monolayer of $1\mu_B$ moments for square and random lattices (solid and dashed lines, respectively). Δ near the monolayer follows eq 2 with α = 3.0 (dotted line). The hatched area indicates the depth where α deviates from its asymptotic value.

molecules, experience a large distribution of magnetic fields, which is attributed to the dipolar fields from the Mn_{12} monolayer.

The observed resonance broadening, depicted in Figure 1c, can be described in terms of dipolar fields from the Mn_{12} moments $\langle \mathbf{m} \rangle = m\hat{z}$, which are preferentially aligned by $\mathbf{H_0}$. For discussion purposes, let us start by assuming that the Mn_{12} moments are arranged in a two-dimensional square lattice with a lattice constant a at $z = -z_0$, where the Si substrate surface is assumed to be at $z = 0$. The z component of the total dipolar field, experienced by a ^{8}Li at $\mathbf{R} = x\hat{x} + y\hat{y} + z\hat{z}$, due to moments m_i at $\mathbf{R_i} = X_i\hat{x} + Y_i\hat{y} - z_0\hat{z}$ is

$$H_z^d(z) = \sum_i \frac{\mu_0 m}{4\pi r_i^3}\left(\frac{3z^2}{r_i^2} - 1\right) \qquad (1)$$

where $\mathbf{r_i} = \mathbf{R} - \mathbf{R_i}$. As we shall see below, it is useful for calculation purposes to parametrize the width of the dipolar field distribution experienced by a ^{8}Li stopping at a depth z with a reasonable analytical function. Simulations indicate that the dipolar fields from the Mn_{12} monolayer decay in the Si according to a power law

$$\Delta(z) = \Delta_0\left(1 + \frac{z}{z_0}\right)^{-\alpha} \qquad (2)$$

where Δ_0 is the width of dipolar field distribution at the surface of the Si substrate ($z = 0$), z_0 is the distance between the monolayer and the Si surface, and α is a parameter describing the decay of dipolar field in the substrate as a function of depth. Note that Δ_0 is proportional to the magnetic moment m. In Figure 2 we plot the results of the simulation for Δ as a function of distance from the plane of the monolayer (solid line). Near the Mn_{12} moments [$(z + z_0) \ll a$] the magnetic field is effectively that of the nearest moment and therefore $H_z^d(z)$ follows the asymptotic behavior for a dipolar field of a single moment, which agrees with eq 2 with α = 3.0 (dotted line). However, for increased stopping depths [$(z + z_0) \sim a$], the field experienced by each ^{8}Li contains significant contributions from several Mn_{12} moments on the surface. This results in cancellations that lead to a faster decrease in the fields (reflected by a deviation from the α = 3.0 power law behavior). Finally, at even greater distances the magnetic field becomes almost uniform, similar to the case of a dipolar field from a uniform magnetic layer.[35] (The small but nonvanishing value of Δ in Figure 2 is due to the finite size of lattice used in the simulations as well as rounding errors.) In our experiment, we expect considerable randomness in the Mn_{12} arrangement in the monolayer.[36] However, simulations show that our conclusions from the model described above are independent of the detailed arrangement of the Mn_{12} moments, since randomness introduces only a reduction in the asymptotic value of α for $(z + z_0) \ll a$ and a slight increase of α and the range of the dipolar fields deeper into the substrate, as can be seen in Figure 2 (dashed line). We point out here that since the implanted ^{8}Li senses mainly the few nearest grafted neighbors (<10 molecules), the simulations which assume a perfect flat substrate are still valid if the surface roughness is small (≪1 nm) within the area occupied by these neighbors. This is the case for our Si substrates, where the roughness is 0.1−0.2 nm over an area of at least 200 × 200 nm.[12,37]

In addition to the obvious broadening at low E, the observed line shape also changes. At high E (bottom of Figure 1c) the line shape fits well to a simple Lorentzian function, while at low E (top of Figure 1c) it has a different shape characterized by a sharp center and broad tails. The intrinsic resonance line shape of ^{8}Li in Si is that obtained at high implantation energy. Therefore, the low implantation energy line shape may be simulated by calculating the broadening of the intrinsic line due to dipolar fields generated by the monolayer. For simplicity we assume that the magnetic field distribution at a depth z in the Si substrate, $n(B, z)$, is a uniform distribution between ±Δ(z) (eq 2). This assumption is necessary due to the lack of knowledge of the exact lattice structure of the grafted Mn_{12} moments on the surface, and therefore it is impossible to simulate the exact form of $n(B, z)$. However, this allows (at least qualitatively) an estimate of the size of dipolar fields as a function of depth. For each implantation energy we calculate a depth-averaged field distribution

$$\langle n(B) \rangle = \int \rho(z) n(B,z)\, dz \qquad (3)$$

where $\rho(z)$ is the stopping distribution obtained using the TRIM.SP code[38,39] to simulate the implantation profile of ^{8}Li in Si. The final step in generating the line shape is to convolute $\langle n(B) \rangle$ by the intrinsic Lorentzian line shape, i.e., the line shape obtained from the high E measurement. Recall, this line shape is identical to that obtained in sample **2**, but it represents a more accurate in situ reference to the low E resonance since it can be measured at exactly the same experimental conditions (temperature, H_1, etc.). The calculated line shape is used to fit the β-NMR spectra, e.g., the solid line in Figure 1c, where Δ_0, α, and z_0 are the fitting parameters.

The best fit of the resonance lines at the implantation energy of E = 1 keV and all temperatures is achieved with

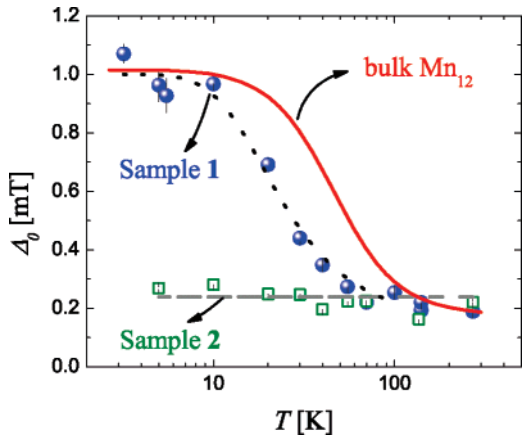

Figure 3. The measured broadening Δ_0 in samples **1** (circles) and **2** (squares) as a function of temperature at $E = 1$ keV. The solid line is the measured m_z in bulk and the dotted line is a guide to the eye. The dashed line represents the average Δ_0 measured in the control sample **2**.

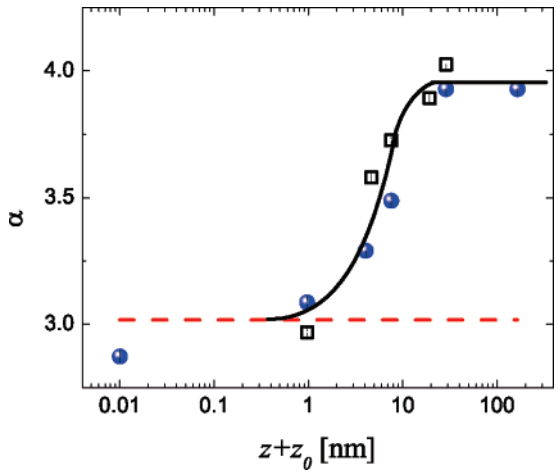

Figure 4. The power law exponent α as a function of implantation depth estimated from fitting the resonances at $T = 3.2$ K (circles) and 5 K (squares). The solid line is a guide to the eye and the dashed line represents the asymptotic value $\alpha = 3.0$ near the monolayer.

a common $\alpha = 3.0 \pm 0.2$ and $z_0 = 1.2 \pm 0.1$ nm, while Δ_0 varies with temperature. In Figure 3 we plot the fitted values of Δ_0 as a function of temperature for both samples **1** (circles) and **2** (squares). At high temperatures the width Δ_0 is small, ∼0.2 mT, and is *equal in both samples*. However, in sample **1** it increases dramatically as the temperature is lowered below ∼100 K reaching ∼1.1 mT at $T = 3.2$ K, while it remains unchanged in sample **2**. Clearly, this temperature-dependent broadening is due to the Mn_{12} magnetic moments at the surface of sample **1**. The small Δ_0 at high temperature in both samples is unrelated to the Mn_{12} magnetic moments, but rather it is likely due to changes in the Si structure near the surface, caused by the grafted ligands and resulting in a small quadrupolar broadening.[24,40,41]

As discussed above, a measurement of Δ_0, or more precisely the difference between the broadening in samples **1** and **2**, as a function of temperature is equivalent to measuring the *z* component of the effective magnetic moment (m_z) of a single Mn_{12} molecule. As shown in Figure 3, there is a sharp increase below ∼100 K and saturation at low temperature. The increase of m_z below ∼100 K is indicative of the gradual depopulation of thermally activated states. The low-temperature saturation occurs when most of the Mn_{12} moments reside in their ground spin state in this 2D configuration and are aligned with the applied magnetic field. We compare the measured magnetization for the monolayer to that measured in a bulk Mn_{12} sample at the same applied field (solid line in Figure 3). The bulk magnetization was scaled to match the low-temperature broadening. Clearly, there is a dramatic difference between our experimental results in the monolayer compared to that in the bulk. This difference is a strong indication that the magnetic properties of Mn_{12} in the 2D configuration are significantly different from the bulk. Earlier studies suggest that the Mn_{12} clusters in the monolayer remain intact.[36] Hence the difference is most probably due to changes in their electronic structure, which may be caused by distortions of the Mn_{12} core in the monolayer due to the different local environment.

Several other points are noteworthy. No shift in the resonance frequency is observed. Simulations show that this is expected due to the randomness in the lattice which acts to reduce the shift to below experimental resolution (<0.05 mT). In addition the value of $z_0 = 1.2 \pm 0.1$ nm, obtained from the fits, is in very good agreement with the thickness of the grafted layer (∼1.1 nm) measured using atomic force lithography.[12] Inspection of the resonance lines at different depths and $T = 3.2$ and 5 K shows that α (obtained from best fits using a common value of Δ_0 and z_0 for each temperature) exhibits a strong dependence on the implantation depth (Figure 4). As expected, we find that at low implantation depth (near the monolayer) $\alpha \approx 3$, with a large deviation at larger depths. The deviation from the asymptotic value $\alpha = 3.0$ begins to occur when the average implantation depth exceed ∼1 nm. Compared with simulations of the dipolar fields of the Mn_{12} moments on the Si substrate, this corresponds to $0.3a-0.5a$ and allows a rough estimate of the average distance between neighboring Mn_{12} molecules of $a \sim 2-3.3$ nm, a reasonable value considering the size of Mn_{12} molecules core.[12] Finally, using the extracted values of a and z_0 to simulate the dipolar field to roughly estimate Δ_0, we find that the low temperature average of $\Delta_0 \sim 1$ mT corresponds to a Mn_{12} magnetic moment of $5\mu_B-12\mu_B$, as expected for an electronic magnetic moment with a large effective spin.

In conclusion, we used β-NMR of ^{8}Li to measure the effective magnetic moment of a single Mn_{12} molecule in a monolayer grafted on Si, demonstrating that the technique has the required sensitivity to investigate the magnetic properties of a submonolayer of magnetic molecules. The temperature dependence of the Mn_{12} magnetic moment indicates that their magnetic properties and spin Hamiltonian are dramatically different from bulk. Since future practical applications of SMMs will undoubtedly require them to be fabricated in the form of monolayers, it is important to understand and thus control any modifications that result from depositing them on surfaces.[42]

Acknowledgment. This work was supported by the CIAR, NSERC, and TRIUMF. We thank Syd Kreitzman, Rahim Abasalti, Bassam Hitti, and Donald Arseneau for technical support.

References

(1) Gatteschi, D.; Sessoli, R. *Angew. Chem., Int. Ed.* **2003**, *42*, 268.
(2) Prokofév, N.; Stamp, P. C. E. *J. Low Temp. Phys.* **1996**, *104*, 143.
(3) Joachim, C.; Gimzewski, J. K.; Aviram, A. *Nature* **2000**, *408*, 541.
(4) Divincenzo, D. In *Quantum Tunneling of the Magnetization—QTM '94*; Gunther, L., Barbara, B., Eds.; Kluwer Publishing: Dordrecht, 1995; p 189.
(5) Tejada, J.; Chudnovsky, E. M.; del Barco, E.; Hernandez, J. M.; Spiller, T. P. *Nanotechnology* **2001**, *12*, 181.
(6) Troiani, F.; Affronte, M.; Carretta, S.; Santini, P.; Amoretti, G. *Phys. Rev. Lett.* **2005**, *94*, 190501.
(7) Troiani, F.; Ghirri, A.; Affronte, M.; Carretta, S.; Santini, P.; Amoretti, G.; Piligkos, S.; Timco, G.; Winpenny, R. E. P. *Phys. Rev. Lett.* **2005**, *94*, 207208.
(8) Cornia, A.; Fabretti, A. C.; Pacchioni, M.; Zobbi, L.; Bonacchi, D.; Caneschi, A.; Gatteschi, D.; Biagi, R.; Pennino, U. D.; Renzi, V. D.; Gurevich, L.; der Zant, H. S. J. V. *Angew. Chem., Int. Ed.* **2003**, *42*, 1645.
(9) Mannini, M.; Bonacchi, D.; Zobbi, L.; Piras, F. M.; Speets, E. A.; Caneschi, A.; Cornia, A.; Magnani, A.; Ravoo, B. J.; Reinhoudt, D. N.; Sessoli, R.; Gatteschi, D. *Nano Lett.* **2005**, *5*, 1435.
(10) Zobbi, L.; Mannini, M.; Pacchioni, M.; Chastanet, G.; Bonacchi, D.; Zanardi, C.; Biagi, R.; Pennino, U. D.; Gatteschi, D.; Cornia, A.; Sessoli, R. *Chem. Commun.* **2005**, 1640.
(11) Naitabdi, A.; Bucher, J.-P.; Gerbier, P.; Rabu, P.; Drillon, M. *Adv. Mater.* **2005**, *17*, 1612.
(12) Condorelli, G. G.; Motta, A.; Fragalà, I. L.; Giannazzo, F.; Raineri, V.; Caneschi, A.; Gatteschi, D. *Angew. Chem., Int. Ed.* **2004**, *43*, 4081.
(13) Fleury, B.; Catala, L.; Huc, V.; David, C.; Zhong, W. Z.; Jegou, P.; Baraton, L.; Palacin, S.; Albouy, P.-A.; Mallah, T. *Chem. Commun.* **2005**, 2020.
(14) Friedman, J. R.; Sarachik, M. P.; Tejada, J.; Ziolo, R. *Phys. Rev. Lett.* **1996**, *76*, 3830.
(15) Thomas, L.; Lionti, F.; Ballou, R.; Gatteschi, D.; Sessoli, R.; Barbara, B. *Nature (London)* **1996**, *383*, 145.
(16) Sangregorio, C.; Ohm, T.; Paulsen, C.; Sessoli, R.; Gatteschi, D. *Phys. Rev. Lett.* **1997**, *78*, 4645.
(17) Wernsdorfer, W.; Sessoli, R. *Science* **1999**, *284*, 133.
(18) Wernsdorfer, W.; et al. *Europhys. Lett.* **2000**, *50*, 552.
(19) Hill, S.; Edwards, R. S.; Aliaga-Alcalde, N.; Christou, G. *Science* **2003**, *302*, 1015.
(20) del Barco, E.; Kent, A. D.; Yang, E. C.; Hendrickson, D. N. *Phys. Rev. Lett.* **2004**, *93*, 157202.
(21) Morello, A.; Stamp, P. C. E.; Tupitsyn, I. S. *Phys. Rev. Lett.* **2006**, *97*, 207206.
(22) Keeler, T. A.; Salman, Z.; Chow, K. H.; Heinrich, B.; Hossain, M. D.; Kardasz, B.; Kiefl, R. F.; Kreitzman, S. R.; MacFarlane, W. A.; Mosendz, O.; Parolin, T. J.; Wang, D. *Physica B* **2006**, *374−375C*, 79.
(23) Morris, G. D.; MacFarlane, W. A.; Chow, K. H.; Salman, Z.; Arseneau, D. J.; Daviel, S.; Hatakeyama, A.; Kreitzman, S. R.; Levy, C. D. P.; Poutissou, R.; Heffner, R. H.; Elenewski, J. E.; Greene, L. H.; Kiefl, R. F. *Phys. Rev. Lett.* **2004**, *93*, 157601.
(24) Salman, Z.; Kiefl, R. F.; Chow, K. H.; Hossain, M. D.; Keeler, T. A.; Kreitzman, S. R.; Levy, C. D. P.; Miller, R. I.; Parolin, T. J.; Pearson, M. R.; Saadaoui, H.; Schultz, J. D.; Smadella, M.; Wang, D.; MacFarlane, W. A. *Phys. Rev. Lett.* **2006**, *96*, 147601.
(25) Salman, Z.; Mansour, A. I.; Chow, K. H.; Beaudoin, M.; Fan, I.; Jung, J.; Keeler, T. A.; Kiefl, R. F.; Levy, C. D. P.; Ma, R. C.; Morris, G. D.; Parolin, T. J.; Wang, D.; MacFarlane, W. A. *Phys. Rev. B* **2007**, *75*, 073405.
(26) Parolin, T. J.; Salman, Z.; Chakhalian, J.; Song, Q.; Chow, K. H.; Hossain, M. D.; Keeler, T.; Kiefl, R. F.; Kreitzman, S. R.; Levy, C. D. P.; Miller, R. I.; Morris, G. D.; Pearson, M. R.; Saadaoui, H.; Wang, D.; MacFarlane, W. A. *Phys. Rev. Lett.* **2007**, *98*, 047601.
(27) Lascialfari, A.; Gatteschi, D.; Borsa, F.; Shastri, A.; Jang, Z.; Carretta, P. *Phys. Rev. B* **1998**, *57*, 514.
(28) Lascialfari, A.; Jang, Z. H.; Borsa, F.; Carretta, P.; Gatteschi, D. *Phys. Rev. Lett.* **1998**, *81*, 3773.
(29) Furukawa, Y.; Watanabe, K.; Kumagai, K.; Borsa, F.; Sasaki, T.; Kobayashi, N.; Gatteschi, D. *Phys. Rev. B* **2003**, *67*, 064426.
(30) Goto, T.; Koshiba, T.; Kubo, T.; Awaga, K. *Phys. Rev. B* **2003**, *67*, 104408.
(31) Morello, A.; Bakharev, O. N.; Brom, H. B.; Sessoli, R.; de Jongh, L. J. *Phys. Rev. Lett.* **2004**, *93*, 197202.
(32) Salman, Z.; Keren, A.; Mendels, P.; Marvaud, V.; Scuiller, A.; Verdaguer, M.; Lord, J. S.; Baines, C. *Phys. Rev. B* **2002**, *65*, 132403.
(33) Salman, Z.; Keren, A.; Mendels, P.; Scuiller, A.; Verdaguer, M. *Physica B* **2000**, *289−290*, 106.
(34) Crane, S. G.; Brice, S. J.; Goldschmidt, A.; Guckert, R.; Hime, A.; Kitten, J. J.; Vieira, D. J.; Zhao, X. *Phys. Rev. Lett.* **2001**, *86*, 2967.
(35) Xu, M.; Hossain, M. D.; Saadaoui, H.; Parolin, T. J.; Chow, K. H.; Keeler, T. A.; Kiefl, R. F.; Morris, G. D.; Salman, Z.; Wang, D.; MacFarlane, W. A. Unpublished.
(36) Condorelli, G. G.; Motta, A.; Favazza, M.; Nativo, P.; Fragalá, I. L.; Gatteschi, D. *Chem. Eur. J.* **2006**, *12*, 3558.
(37) Condorelli, G. G.; Motta, A.; Favazza, M.; Fragalà, I. L.; Busi, M.; Menozzi, E.; Dalcanale, E.; Cristofolini, L. *Langmuir* **2006**, *22*, 11126.
(38) Eckstein, W. *Computer Simulation of Ion-Solid Interactions*; Springer: Berlin, Heidelberg, New York, 1991.
(39) Morenzoni, E.; Glucker, H.; Prokscha, T.; Khasanov, R.; Luetkens, H.; Birke, M.; Forgan, E. M.; Niedermayer, C.; Pleines, M. *Nucl. Instrum. Methods Phys. Res.* **2002**, *192*, 254.
(40) Salman, Z.; Reynard, E. P.; MacFarlane, W. A.; Chow, K. H.; Chakhalian, J.; Kreitzman, S. R.; Daviel, S.; Levy, C. D. P.; Poutissou, R.; Kiefl, R. F. *Phys. Rev. B* **2004**, *70*, 104404.
(41) Salman, Z.; Kiefl, R. F.; Chow, K. H.; MacFarlane, W. A.; Kreitzman, S. R.; Arseneau, D. J.; Daviel, S.; Levy, C. D. P.; Maeno, Y.; Poutissou, R. *Physica B* **2006**, *374−375C*, 468.
(42) Jo, M.-H.; Grose, J.; Baheti, K.; Deshmukh, M.; Sokol, J.; Rumberger, E.; Hendrickson, D.; Long, J.; Park, H.; Ralph, D. *Nano Lett.* **2006**, *6*, 2014.

NL070366A